Roughness exponent in the Domany-Kinzel cellular automaton

1999 J. Phys. A: Math. Gen. 32 885

(http://iopscience.iop.org/0305-4470/32/6/003)

J. Phys. A: Math. Gen. **32** (1999) 885–890. Printed in the UK PII: S0305-4470(99)97751-X

Roughness exponent in the Domany–Kinzel cellular automaton

J A de Sales†, M L Martins‡ and J G Moreira†

† Departamento de Física, Instituto de Ciências Exatas, Universidade Federal de Minas Gerais, CP 702, 30161-970, Belo Horizonte, MG, Brazil

‡ Departamento de Física, Universidade Federal de Viçosa, 36571-000, Viçosa, MG, Brazil

Received 21 September 1998

Abstract. We propose a method to detect phase transitions in discrete lattice models based on the roughness exponent. This approach is applied to the one-dimensional Domany–Kinzel cellular automaton (CA). Our results, obtained by numerical simulations, show that the roughness exponent method detects the frozen–active phase transition directly from the CA spatio-temporal configurations without any reference to thermodynamical potentials, order parameters or response functions.

The Hurst or roughness exponent is one of the standard tools used to describe various roughening processes observed in the field of disordered surface growth [1]. The roughness exponent was largely used as a method for obtaining the fractal characteristics of biological structures and time-varying signals such as DNA sequences [2], heart rates, respiratory rates and neural pulse trains [3]. The central goal of this approach is to provide information about the correlations between the fluctuations of a space varying property. Recently, we have used the roughness exponent concept to classify the Wolfram cellular automata [4].

In this paper we apply the roughness exponent analysis to the one-dimensional Domany–Kinzel probabilistic cellular automaton (DK-PCA). It is the simplest locally interacting statistical model which exhibits a second-order phase transition from a empty (or frozen) state to a partially occupied (or active) state. It exhibits also a continuous damage-spreading phase transition.

The one-dimensional DK-PCA [5] consists of a linear chain of N lattice sites ($i = 1, 2, \ldots, N$), with periodic boundary conditions. Each site has two possible states $\sigma_i = 0, 1$. The state of the system at time t is specified by the set $\{\sigma_i\}$. At the next time step, the state of a given site is $\sigma_i(t+1) = 0$ or 1 according to the conditional probabilities $\{p(\sigma_{i-1}(t), \sigma_i(t)/\sigma_i(t+1))\}$, i.e. $p_0 \equiv p(00/1)$, $p_1 \equiv p(10/1) = p(01/1)$ (isotropic case) and $p_2 \equiv p(11/1)$. Naturally $p(\sigma_{i-1}, \sigma_i/0) = 1 - p(\sigma_{i-1}, \sigma_i/1)$. The DK-PCA contains, as special cases, the problem of directed percolation and directed compact percolation [6, 7] on the square lattice.

Domany and Kinzel showed that this PCA presents a continuous transition between a 'frozen' phase in which all the sites are in the empty state and an 'active' phase characterized by a constant average fraction of sites in the active state ($\sigma_i = 1$). Later, Martins *et al* [8] found, by using the damage-spreading method, that the active phase is divided into two regions: one in which the system exhibits sensitivity to the initial conditions (chaotic phase) and another in

0305-4470/99/060885+06$19.50

which it does not. They also showed that the transition between those regions is a continuous one. Recently, Hinrichsen *et al* [9] demonstrated that, indeed, the active phase is subdivided into three dynamical phases, namely: (i) the chaotic phase of Martins *et al* in which the damage spreads for all possible types of correlated noise used to update the two replica systems; (ii) a phase in which the damage spreads only for some types of noise; and, finally, (iii) a region in which the damage always disappears.

As shown in an earlier work [4], CA evolution patterns can be mapped on random walk-like profiles which are self-affine. Thus, the roughness exponents associated to these profiles also characterize the spatio-temporal patterns generated by CA rule and, therefore, can be used as an additional statistical measure of correlations present in CA configurations. Self-affine profiles can be generated by CA evolution using various methods. The simplest of them is the 1:1 mapping between a given CA configuration at time t and a 'walk process' [2]. In this method each binary symbol $\sigma_i(t)$ is identified with a step (to the right or to the left) of a one-dimensional walk. Specifically, to a unique CA configuration $\{\sigma_1(t), \sigma_2(t), \ldots, \sigma_N(t)\}$ at fixed time t corresponds a spatial profile, $\{h_1(t), h_2(t), \ldots, h_N(t)\}$, given by the sequence of the walker displacements h_i after i unit steps defined as

$$h_i(t) = \sum_{j=1}^{i} [2\sigma_i(t) - 1]. \tag{1}$$

Another method consists of accumulating (or sum) all the values assumed by the variables $\sigma_i(t)$ during a given number τ of successive time steps

$$h_i(\tau) = \sum_{t=t_0}^{t_0+\tau} \sigma_i(t) \tag{2}$$

$i = 1, 2, \ldots, N$. Thus, $h_i(\tau)$ specifies the profile height at time $t_0 + \tau$ at site i, in analogy with solid on solid growth models in 1 + 1 dimensions [12].

After obtaining the profiles, the nature of their correlations could be investigated through the analysis of the profile roughness [10]. Since the profiles generated by DK-PCA evolution usually have drifts, we use the method of roughness around the root mean square straight line [11] to evaluate the roughness exponent H. In this method, the roughness $W(N, \epsilon)$ in the scale ϵ is given by

$$W(N, \epsilon, t) = \frac{1}{N} \sum_{i=1}^{N} w_i(\epsilon, t) \tag{3}$$

and the local roughness $w_i(\epsilon)$ is defined as

$$w_i(\epsilon, t) = \sqrt{\frac{1}{2\epsilon + 1} \sum_{j=i-\epsilon}^{i+\epsilon} \{h_j(t) - [a_i(\epsilon)x_j + b_i(\epsilon)]\}^2}. \tag{4}$$

$a_i(\epsilon)$ and $b_i(\epsilon)$ are the linear fitting coefficients to the displacement data on the interval $[i - \epsilon, i + \epsilon]$ centred on the site i. Self-affine profiles satisfy the scaling law

$$W(\epsilon) \sim \epsilon^H. \tag{5}$$

The exponent H is restricted to the interval [0, 1] and is related to the fractal dimension D of the profile [10]. The general relationship is $H = E + 1 - D$, where E is the Euclidean dimension of the profile ($E = 1$ in this case).

The roughness W can distinguish two possible types of profile. If the 'landscape' is random, or even exhibits a finite correlation length extending up to a characteristic range (such as in Markov chains), then $W \sim N^{1/2}$ as in a normal random walk. In contrast, if there is no

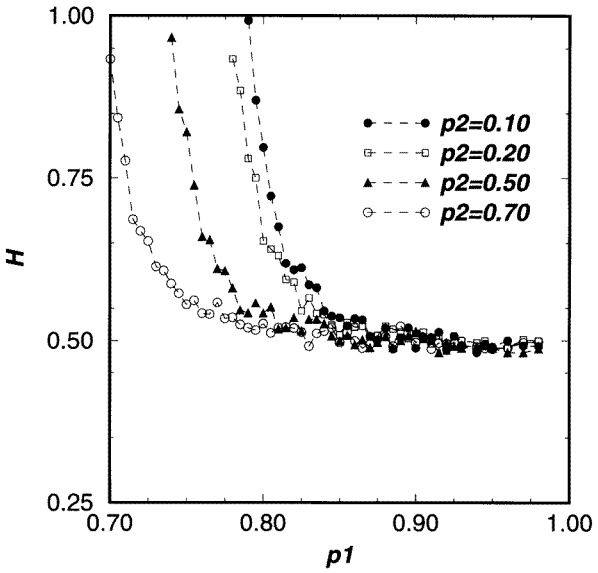

Figure 1. The roughness exponent H as a function of p_1 for four different paths (fixed p_2 values) in the DK-PCA parameter space. Two of them ($p_2 = 0.10$ and 0.20) traverse the active–chaotic critical surface, while the other two ($p_2 = 0.50$ and 0.70) are entirely contained in the non-chaotic active phase. The p_1 ranges in which H changes from 1 to 0.5 are in good agreement with the frozen–active critical surface determined through extensive numerical simulations [13].

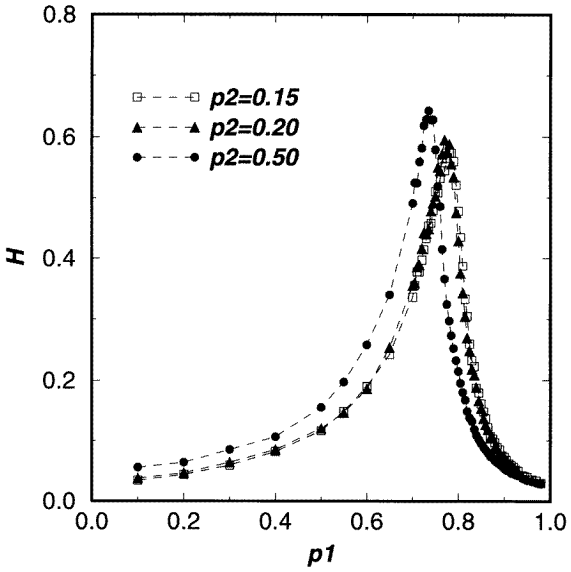

Figure 2. The same as in figure 1 but for profiles obtained using the accumulation method. The frozen–active critical surface corresponds to the p_1 values for which H exhibits a maximum. In contrast, no additional peak associated to the active–chaotic phase transition is observed.

characteristic length (infinitely long-range correlations) then the roughness will be described by a power law with an exponent $H \neq \frac{1}{2}$. $H > \frac{1}{2}$ implies that the profile exhibits persistent

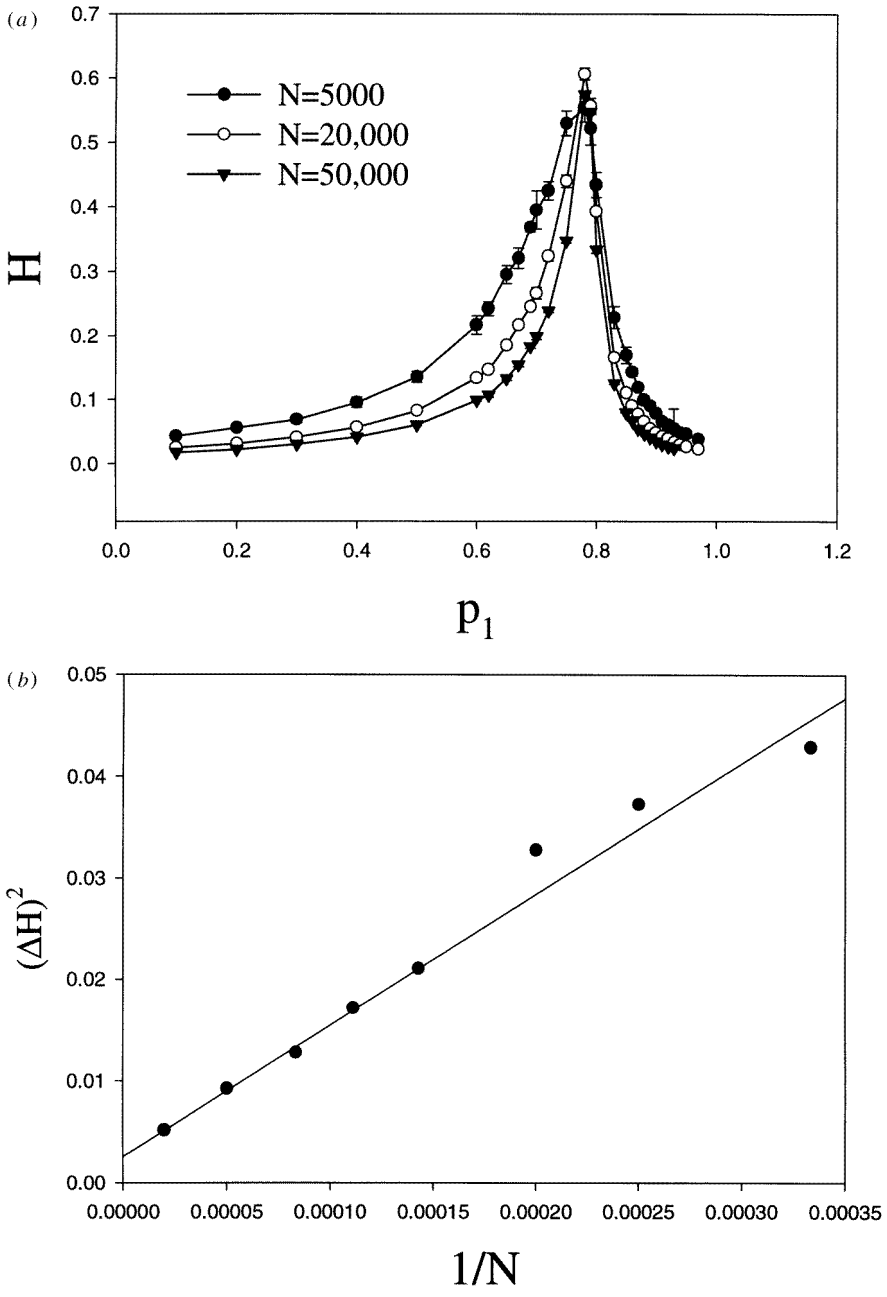

Figure 3. (*a*) Curves $H(p_1)$ and (*b*) their widths ΔH for fixed $p_2 = 0.20$ and various lattice sizes N. For each curve, ΔH was defined as the length of the p_1 interval for which the H values at both of its endpoints correspond to half of the maximum H observed in the curve.

correlations, i.e. a sequence of increases in displacement values is more likely to be followed by subsequent increases and, similarly, decreases are more likely to be followed by subsequent decreases. On the other hand, profiles with $H < \frac{1}{2}$ are anticorrelated, which means that

increases in displacement values are more likely to alternate with subsequent decreases and vice versa.

In figures 1 and 2 our results for the roughness exponents characterizing the configurations generated by the DK-PCA along selected paths of its parameter space are shown. These results correspond to averages over many (typically $\sim$50) random initial configurations taken after a 10 000 time steps transient in CAs containing $N = 4000$ sites. The profiles studied in figure 1 were obtained applying the 'random walk' method. On the other hand, the self-affine profiles analysed in figure 2 were obtained applying the accumulation method on long temporal sequences (up to 15 000 time steps) of length τ beginning from the initial state. Since in the frozen phase the DK-PCA evolution is attracted to an absorbing homogeneous empty state, the corresponding profiles are smooth, with roughness exponent $H = 1$, as shown in figure 1, and fractal dimension $D = 1$. Figure 1 also shows that in the active phase the DK-PCA generates random spatial and temporal profiles (roughness exponents $H = 0.5$) such as the Wolfram rule 90 [4], the deterministic limit $p_1 = 1$, $p_2 = 0$ of the DK-PCA. The parameter ranges in which H changes from 1 to 0.5 are in good agreement with the frozen–active critical surface determined through extensive numerical simulations [13]. However, in figure 1 no perceptible difference is observed among those curves $H(p_1)$ which cross the active–chaotic critical surface and those restricted to the non-chaotic active phase. Thus, the roughness exponent method directly applied to the CA spatial configurations cannot detect the dynamical phase transition exhibited by the DK-PCA. Also, as shown in figure 2, the roughness exponent exhibits a pronounced maximum at the frozen–active critical surface. The small values of H inside the frozen and active phases, indicating the absence of long range correlations, can be understood in terms of deposition processes. As it is well known for non-correlated SOS models [10], the measure of the roughness exponent in a given time results in a value which decreases towards zero with time. Again, there is no evidence for the active–chaotic transition in $H(p_1)$ curves.

A finite size analysis indicates that the smooth peak as well as the continuous decrease observed in the $H(p_1)$ curves in figures 1 and 2 become singular in the thermodynamical limit. Figure 3 shows these curves and their corresponding widths for increasing N. In particular, figure 3(b) shows that the curve widths tend to zero as $N \to \infty$. Thus, the smooth peaks of figure 2 converge to a delta distribution in the asymptotic limit. Similarly, the monotonic decrease of H exhibited in figure 1 tends to a sudden jump from $H = 1$ to $H = \frac{1}{2}$ at the critical p_1 value for infinite lattice sizes.

Finally, it is important to notice that the active–chaotic phase transition can be detected if the roughness exponent method is applied to the 'difference' configurations $\{\eta_i(t) = \sigma_i(t)\ XOR\ \tau_i(t)\}$ associated to two distinct replicas of the DK-PCA whose states $\{\sigma_i(t)\}$ and $\{\tau_i(t)\}$ evolve under the same noise. Thus, dynamical or damage spreading phase transitions cannot be detected only taking into account the spatio-temporal configurations of a single system.

In summary, we have shown that the roughness exponent is able to detect equilibrium phase transitions and provides accurate numerical determination of the critical surfaces without any reference to thermodynamical potentials, order parameters or response functions. Now, we are extending the present analysis to other standard spin models of statistical mechanics. Our first results show that the first and second order phase transitions of the Ising and q-state Potts models are detected by the roughness exponent method, which gives additional support to the generality of this method. All these results will be reported in a future paper.

Acknowledgments

We thank A T Bernardes and J A Plascak for helpful criticism of the manuscript. We acknowledge the partial support given to this work by FAPEMIG (Fundação de Amparo à Pesquisa do Estado de Minas Gerais) and CNPq (Conselho Nacional de Desenvolvimento Científico e Tecnológico), Brazilian agencies. We also thank an anonymous referee for the valuable remarks that improve the paper.

References

[1] Family F and Vicsek T (ed) 1991 *Dynamics of Fractal Surfaces* (Singapore: World Scientific)
[2] Peng C K, Buldyrev S V, Goldberger A L, Havlin S, Sciortino F, Simons M and Stanley H E 1992 *Nature* **356** 168
Stanley H E, Buldyrev S V, Goldberger A L, Goldberger Z D, Havlin S, Mantegna R N, Ossadnik S M, Peng C K and Simons M 1994 *Physica* A **205** 214
[3] Bassingthwaighte J B, Liebovitch L S and West B J 1994 *Fractal Physiology* (New York: Oxford University Press)
[4] Sales J A, Martins M L and Moreira J G 1997 *Physica* A **245** 461
[5] Domany E and Kinzel W 1984 *Phys. Rev. Lett.* **53** 447
Kinzel W 1985 *Z. Phys.* B **58** 229
[6] Essam J W 1989 *J. Phys. A: Math. Gen.* **22** 4927
[7] Essam J W and Tanlakishani W 1987 *Disorder in Physical Systems* ed G R Grimmett and D J A Welsh (Oxford: Oxford University Press)
[8] Martins M L, Verona de Resende H F, Tsallis C and de Magalhães A C N 1991 *Phys. Rev. Lett.* **66** 2045
[9] Hinrichsen H, Weitz J S and Domany E 1997 *J. Stat. Phys.* **88** 617
[10] Barabási A L and Stanley H E 1995 *Fractal Concepts in Surface Growth* (Cambridge: Cambridge University Press)
[11] Moreira J G, Kamphorst Leal da Silva J and Oliffson Kamphorst S 1994 *J. Phys. A: Math. Gen.* **27** 8079
[12] Family F 1990 *Physica* A **168** 441
[13] Zebende G F and Penna T J P 1994 *J. Stat. Phys.* **74** 1273